

# Theoretical Investigation on the Mechanisms of the PtCl<sub>2</sub>-Mediated Cycloisomerization of Polyfunctionalized 1,6-Enynes. 2. Propargylic Carboxylates

Elena Soriano,<sup>\*,†</sup> Paloma Ballesteros,<sup>†</sup> and José Marco-Contelles<sup>\*,‡</sup>

Laboratorio de Síntesis Orgánica e Imagen Molecular por Resonancia Magnética, Instituto Universitario de Investigación, UNED, Senda del Rey, 9, 28040-Madrid, Spain, and Laboratorio de Radicales Libres, IQOG (CSIC), C/ Juan de la Cierva 3, 28006-Madrid, Spain

Received February 23, 2005

The PtCl<sub>2</sub>-mediated cycloisomerization of hept-1-en-6-yne functionalized at propargylic positions shows a high versatility and may afford different kinds of products. On the basis of a broad DFT computational study, mechanistic understandings of these processes are provided. The results suggest that these reactions could proceed through cyclopropyl platinum carbenes formed by endo or by exo cyclization routes. The role of the propargylic substituent and the additional alkene chain for diene precursors in the course of each type of cycloisomerization is discussed. Thus, although the metathesis process and formation of polycyclic adducts involves an initial 5-exo cyclopropanation path, a propargylic acyl group promotes the formation of bicyclic enol esters by an initial endo cyclopropanation, followed by [1,2]-acyl migration. This bulky propargylic group also inhibits other cycloisomerization reactions due to steric interactions, such as the Alder-ene process, and simultaneously allows an easy [1,2]-acyl migration by anchimeric assistance to yield bicyclic [*n*.1.0] enol esters.

## Introduction

In the last few years, the transition-metal-catalyzed cycloisomerization of 1,6-enynes has become a powerful methodology for the synthesis of a variety of carbo- or heterocycles.<sup>1</sup> Intriguingly, several transformations are possible for these kinds of substrates, and they may give rise to metathesis products,<sup>2,3</sup> Alder-ene adducts,<sup>4,5</sup> and formation of diverse cyclopropyl derivatives.<sup>6</sup> Thus, it

has been observed that minor changes of the reaction conditions and/or substrate structures can lead to completely different products.

In this context, a very interesting study by Marco-Contelles, Malacria, Fensterbank, et al. has reported the cyclization of precursors bearing a free or protected hydroxy group at the propargylic position. The results clearly show that the nature of the propargylic substituent critically controls the evolution of the processes. Thus, depending on the type or absence of this protecting group, skeletal rearrangement, stereoselective tetraacyclic compounds, or bicyclic [4.1.0] enol esters are isolated.<sup>7</sup>

Because of the high versatility, further insights into the mechanistic aspects and the role of the propargylic substituent in the evolution of the catalytic processes are desirable, to develop new useful synthetic strategies. Thus, as a part of an extensive study of PtCl<sub>2</sub>-mediated cycloisomerizations of diverse polyunsaturated systems,<sup>8</sup> we present a detailed DFT analysis to elucidate the molecular mechanisms and identify the factors that selectively lead to the cycloisomerizations shown in Scheme 1. Herein, we wish to focus our attention on the mechanism of formation of bicyclic enol esters from propargylic carboxylates. We have discussed the effects of other propargylic substituents elsewhere.<sup>8a,9</sup>

(6) (a) Blum, J.; Beerkraft, H.; Badrieh, Y. *J. Org. Chem.* **1995**, *60*, 5567–5569. (b) Fürstner, A.; Szillat, H.; Stelzer, F. *J. Am. Chem. Soc.* **2000**, *122*, 6785–6786. (c) Fürstner, A.; Stelzer, F.; Szillat, H. *J. Am. Chem. Soc.* **2001**, *123*, 11863–11869. (d) Méndez, M.; Muñoz, M. P.; Nevado, C.; Cárdenas, D. J.; Echavarren, A. M. *J. Am. Chem. Soc.* **2001**, *123*, 10511–10520.

(7) Mainetti, E.; Mouries, V.; Fensterbank, L.; Malacria, M.; Marco-Contelles, J. *Angew. Chem., Int. Ed.* **2002**, *41*, 2132–2135.

(8) (a) Soriano, E.; Ballesteros, P.; Marco-Contelles, J. *J. Org. Chem.* **2004**, *69*, 8018–8023. (b) Soriano, E.; Marco-Contelles, J. *Chem. Eur. J.* **2005**, *11*, 521–533.

\* To whom correspondence should be addressed. E-mail: esoriano@arrakis.es (E.S.); iqoc21@iqog.csic.es (J.M.-C.).

† UNED.

‡ IQOG (CSIC).

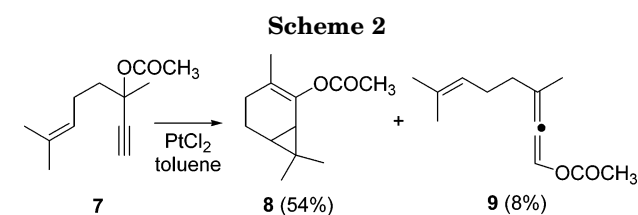
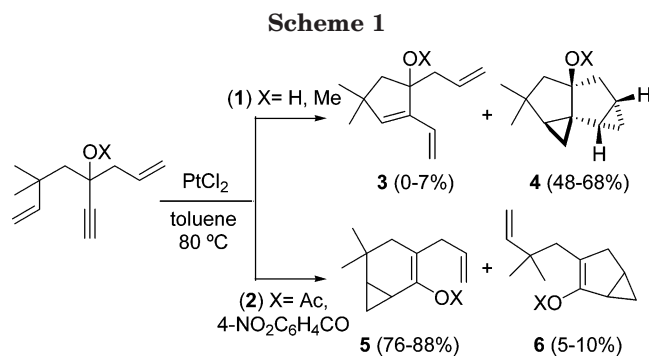
(1) (a) Trost, B. M.; Krische, M. J. *Synlett* **1998**, 1–16. (b) Trost, B. M.; Toste, F. D.; Pinkerton, A. B. *Chem. Rev.* **2001**, *101*, 2067–2096. (c) Aubert, C.; Buisine, O.; Malacria, M. *Chem. Rev.* **2002**, *102*, 813–834. (d) Lloyd-Jones, G. C. *Org. Biomol. Chem.* **2003**, *1*, 215–236.

(2) (a) Diver, S. T.; Giessent, A. *J. Chem. Rev.* **2004**, *104*, 1317–1382. (b) Mori, M. In *Topics in Organometallic Chemistry*; Fürstner, A., Ed.; Springer-Verlag: Berlin, 1998; Vol. 1, p 133. (c) Fürstner, A. *Angew. Chem., Int. Ed.* **2000**, *39*, 3012–3043. (d) Poulsen, C. S.; Madsen, R. *Synthesis* **2003**, 1–18.

(3) (a) Trost, B. M.; Tanoury, G. J. *J. Am. Chem. Soc.* **1987**, *109*, 4753–4755. (b) Trost, B. M.; Yanai, M.; Hoogsteen, K. *J. Am. Chem. Soc.* **1993**, *115*, 5294–5295. (c) Fürstner, A.; Szillat, H.; Gabor, B.; Mynott, R. *J. Am. Chem. Soc.* **1998**, *120*, 8305–8314. (d) Trost, B. M.; Doherty, G. A. *J. Am. Chem. Soc.* **2000**, *122*, 3801–3810. (e) Oi, S.; Tsukamoto, I.; Miyano, S.; Inoue, Y. *Organometallics* **2001**, *20*, 3704–3709. (f) Chatani, N.; Inoue, H.; Morimoto, T.; Muto, T.; Murai, S. *J. Org. Chem.* **2001**, *66*, 4433–4436.

(4) Formation of carbocyclic compounds: (a) Trost, B. M.; Lautens, M.; Chan, C.; Jebaratnam, D. J.; Mueller, T. *J. Am. Chem. Soc.* **1991**, *113*, 636–644. (b) Trost, B. M.; Li, Y. *J. Am. Chem. Soc.* **1996**, *118*, 6625–6633. (c) Trost, B. M.; Krische, M. J. *J. Am. Chem. Soc.* **1999**, *121*, 6131–6141. (d) Trost, B. M.; Corte, J. R.; Gudiksen, M. S. *Angew. Chem., Int. Ed.* **1999**, *38*, 3662–3664. (e) Takayama, Y.; Okamoto, S.; Sato, F. *J. Am. Chem. Soc.* **1999**, *121*, 3559–3560. (f) Trost, B. M.; Haffner, C. D.; Jebaratnam, D. J.; Krische, M. J.; Thomas, A. P. *J. Am. Chem. Soc.* **1999**, *121*, 6183–6192.

(5) Formation of heterocyclic compounds: (a) Trost, B. M.; Pedregal, C. *J. Am. Chem. Soc.* **1992**, *114*, 7292–7294. (b) Goeke, A.; Sawamura, M.; Kuwano, R.; Ito, Y. *Angew. Chem., Int. Ed. Engl.* **1996**, *35*, 662–663. (c) Lei, A.; Waldkirch, J. P.; He, M.; Zhang, X. *Angew. Chem., Int. Ed.* **2002**, *41*, 4526–4529.

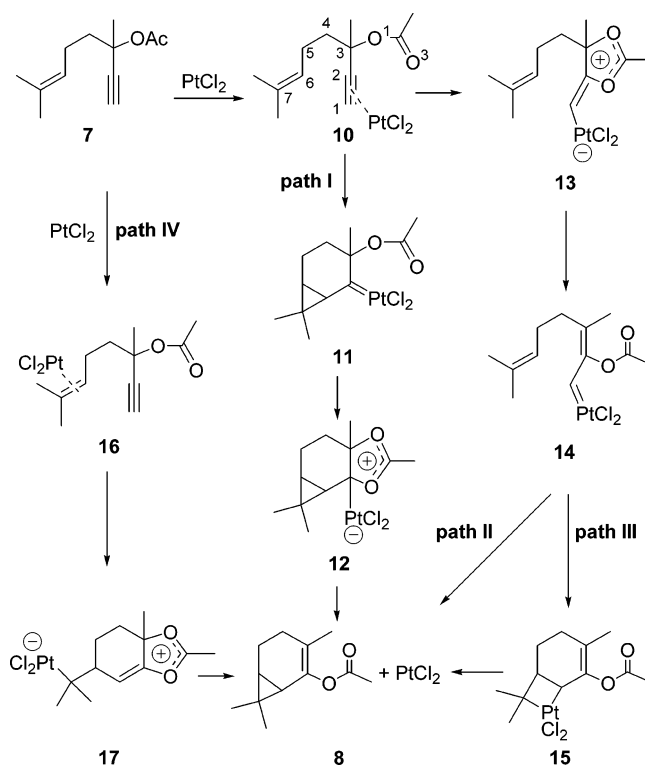


Transition-metal-promoted cycloisomerization of propargylic carboxylates is a very attractive reaction, as it may lead to differently functionalized bicyclo[*n*.1.0]-alkane enol esters (*n* = 3, 4).<sup>10–13</sup> Rautenstrauch described a pioneering similar transformation and proposed that it proceeds via an acetoxonium or butenodienylcarbene intermediate.<sup>14</sup> More recently, Ohe and Uemura have reported the intermolecular version of this reaction, suggesting the involvement of vinylcarbene complexes as key intermediates.<sup>15</sup> However, the actual reaction pathway remains uncertain. Formation of a bicyclo[4.1.0]hept-4-ene framework from 1,6-enyne would suggest an initial 6-endo cyclization to afford a cyclopropylcarbene,<sup>8a</sup> which then could easily undergo a [1,2]-acyl migration to yield the unsaturated bicyclic structure. An inverse sequence of steps should also be conceivable: i.e., initial acyl migration by anchimeric assistance to form a platinum carbene intermediate that subsequently would cyclize, by trapping the alkene.<sup>7,12,13,15</sup>

## Results and Discussion

A wide experimental study aimed at establishing the scope and generality of the PtCl<sub>2</sub>-catalyzed cycloisomerization of unsaturated propargylic carboxylates has shown<sup>10</sup> that, under the standard conditions, the enyne **7** afforded compounds **8** and **9** (Scheme 2). Although **9** was isolated in poor yield, the allenyl esters are routinely found in the transition-metal-catalyzed isomerization of propargylic acetates.<sup>16</sup> On the other hand, and

## Scheme 3. Possible Reaction Pathways for the Transformation of **7** into **8**



very interestingly, no product was detected from the Alder-ene reaction.

In principle, several reaction pathways can be proposed for the transformation of **7** into **8** (Scheme 3). Transition-metal-catalyzed intramolecular cyclizations of 1,6-enynes may proceed via an initial 6-endo (or 5-exo) cyclopropanation step, upon activation of the triple bond by electrophilic catalysts, to afford cyclopropyl Pt-carbene structures. These intermediates have been proposed from experimental evidence<sup>7,17,18</sup> and theoretical calculations<sup>6d,8a,9,19</sup> for related cycloisomerizations of enynes. Then, a plausible [1,2]-acyl migration process could yield the subsequent enol ester (path I of Scheme 3). Alternatively, it has been suggested<sup>7</sup> that the process could take place by initial acyl migration from the propargylic position to the  $\beta$ -carbon center, followed by a concerted addition of the vinyl platinumcarbene to the alkene (path II of Scheme 3). In connection with this mechanistic picture, it has been proposed that related metallacarbenes would intramolecularly add to alkenes to form cyclopropane adducts.<sup>17b,c</sup> Instead, **14** could give a [2 + 2] cycloaddition to form **15**, which would yield the cyclopropane structure by reductive elimination<sup>20</sup>

(9) Soriano, E.; Ballesteros, P.; Marco-Contelles, J. *Organometallics* **2005**, *24*, 3172.

(10) Anjum, S.; Marco-Contelles, J. *Tetrahedron* **2005**, *61*, 4793–4803.

(11) Strickler, H.; Davis, J. B.; Ohloff, G. *Helv. Chim. Acta* **1976**, *59*, 1328–1332.

(12) (a) Mamane, V.; Gress, T.; Krause, H.; Fürstner, A. *J. Am. Chem. Soc.* **2004**, *126*, 8654–8655. (b) Fürstner, A.; Hannen, P. *Chem. Commun.* **2004**, 2546–2547.

(13) Harrak, Y.; Blaszykowski, C.; Bernard, M.; Caroiu, K.; Mainetti, E.; Mourès, V.; Dhimane, A.-L.; Fensterbank, L.; Malacria, M. *J. Am. Chem. Soc.* **2004**, *126*, 8656–8657.

(14) Rautenstrauch, V. *J. Org. Chem.* **1984**, *49*, 950–952.

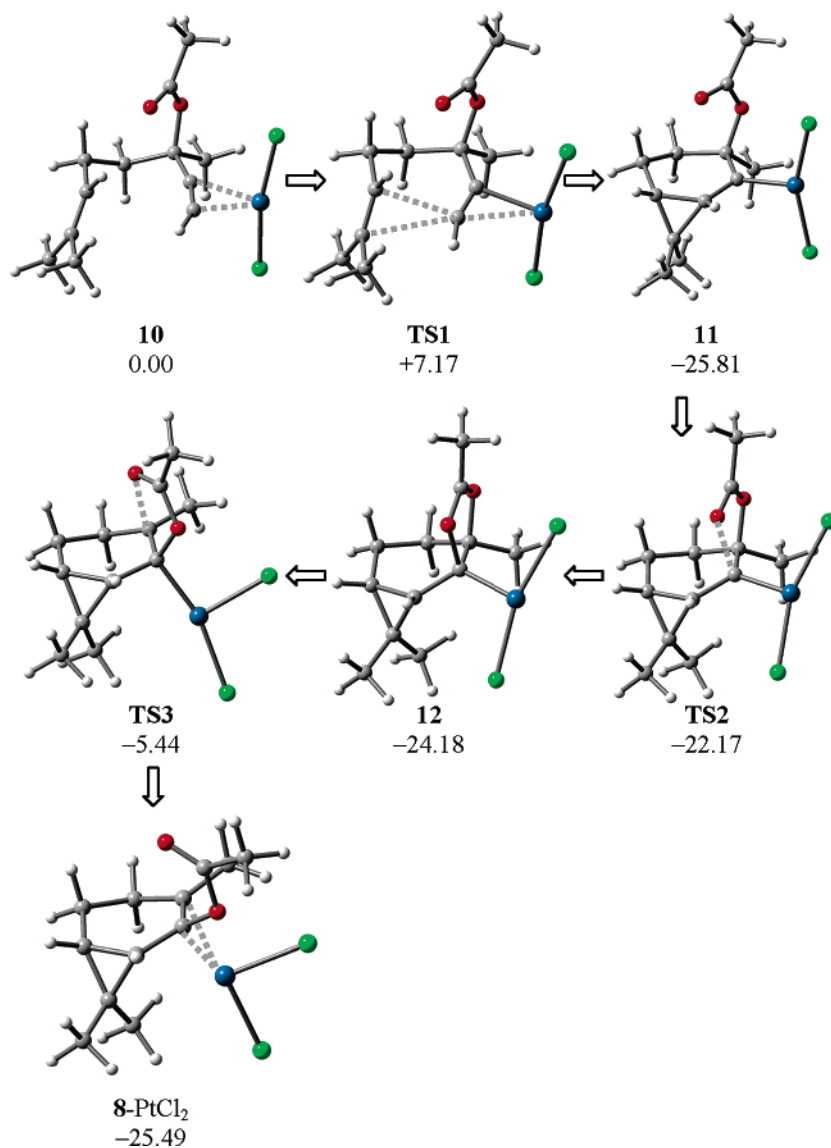
(15) (a) Miki, K.; Ohe, K.; Uemura, S. *Tetrahedron Lett.* **2003**, *44*, 2019–2022. (b) Miki, K.; Ohe, K.; Uemura, S. *J. Org. Chem.* **2003**, *68*, 8505–8513. (c) Miki, K.; Yokoi, T.; Nishino, F.; Kato, Y.; Washitake, Y.; Ohe, K.; Uemura, S. *J. Org. Chem.* **2004**, *69*, 1557–1564.

(16) (a) Silver salts as catalysts: Oelberg, D. G.; Schiavelli, M. D. *J. Org. Chem.* **1977**, *42*, 1804–1806. (b) Cookson, R. C.; Cramp, M. C.; Parsons, P. J. *J. Chem. Soc., Chem. Commun.* **1980**, 197–198. (c) Palladium catalyst: Okumoto, H.; Nishihara, S.; Nakagawa, H.; Suzuki, A. *Synlett* **2002**, 217–218. (d) Kato, K.; Yamamoto, Y.; Akita, H. *Tetrahedron Lett.* **2002**, *43*, 6587–6590.

(17) (a) Trost, B. M.; Hashmi, A. S. K. *Angew. Chem., Int. Ed. Engl.* **1993**, *32*, 1085–1087. (b) Chatani, N.; Kataoka, K.; Murai, S.; Furukawa, N.; Seki, Y. *J. Am. Chem. Soc.* **1998**, *120*, 9104–9105. (c) Nieto-Oberhuber, C.; Muñoz, M. P.; Buñuel, E.; Nevado, C.; Cárdenas, D. J.; Echavarren, A. M. *Angew. Chem., Int. Ed.* **2004**, *43*, 2402–2408.

(18) For recent reviews, see: (a) Bruneau, C. *Angew. Chem., Int. Ed.* **2005**, *44*, 2328–2334. (b) Echavarren, A. M.; Nevado, C. *Chem. Soc. Rev.* **2004**, *33*, 431–436.

(19) Nevado, C.; Cárdenas, D. J.; Echavarren, A. *Chem. Eur. J.* **2003**, *9*, 2627–2635.

**Scheme 4. Optimized Structures for the Reaction Pathway of the PtCl<sub>2</sub>-Mediated Intramolecular Cyclization of 4-*O*-Acetyl-1,6-enyne **7** to the Bicyclo[4.1.0]heptane Derivative **8****

(path III of Scheme 3). Finally, formation of **8** from transition-metal-catalyzed reactions has also been described by other authors, and a conceivable mechanistic proposal based on the initial  $\eta^2$  complexation of the alkene onto the catalyst (path IV of Scheme 3) has been suggested.<sup>11</sup>

Initially, we explored path I and, thus, coordination of PtCl<sub>2</sub> to the alkyne forms the  $\eta^2$  complex **10** (path I of Scheme 3 and Scheme 4). The optimized geometry shows a slightly distorted T-shaped tricoordinated complex. Both chloride atoms are trans arranged, and the alkyne ligand lies nearly perpendicular to the coordination plane. The reactant complex evolves to the cyclopropyl Pt–carbene **11** by concerted nucleophilic anti addition of alkene onto the terminal carbon C<sub>1</sub> of the activated alkyne. This transformation takes place through the early and highly asymmetric transition state **TS1** (C<sub>1</sub>–C<sub>6</sub> = 2.419 and C<sub>1</sub>–C<sub>7</sub> = 2.709 Å). The

short Pt–C<sub>2</sub> bond in **11** (1.872 Å) is consistent with a Pt(II)–carbene nature,<sup>21</sup> though there is a lack of coplanarity between coordination and carbene planes (84–95°), which is due to the presence of substituents at the propargylic position. The formation of **11** is highly exothermic (–25.81 kcal mol<sup>-1</sup>, Figure 1) and proceeds with a low activation energy (7.17 kcal mol<sup>-1</sup>), which points out an easy and favorable transformation from both thermodynamic and kinetic perspectives.

In this way, it is straightforward that a following 1,2-migration of the acetoxy group should afford the enol ester **8**. We found the transition state **TS2** by intramolecular nucleophilic attack of the carbonyl oxygen atom on the electrophilic carbene<sup>22</sup> atom (NPA charges at O<sub>3</sub> and C<sub>2</sub> in **11** –0.605 and +0.169; see Table S3 in the Supporting Information). IRC calculations revealed that **TS2** drives to the polarized intermediate **12** (10.05 D

(20) (a) Casey, C. P.; Hornung, N. L.; Kosar, W. P. *J. Am. Chem. Soc.* **1987**, *109*, 4908–4916. (b) Van Koppen, P. A. M.; Jacobson, D. B.; Illies, A.; Bowers, M. T.; Hanratty, M.; Beauchamp, J. L. *J. Am. Chem. Soc.* **1989**, *111*, 1991–2001.

(21) (a) Cave, G. W. V.; Hallett, A. J.; Errington, W.; Rourke, J. P. *Angew. Chem., Int. Ed.* **1998**, *37*, 3270–3272. (b) Cucciolito, M. E.; Panunzi, A.; Ruffo, F.; Albano, V. G.; Monari, M. *Organometallics* **1999**, *18*, 3482–3489. (c) Jones, N. D.; Lin, G.; Gossage, R. A.; McDonald, R.; Cavell, R. G. *Organometallics* **2003**, *22*, 2832–2841.

(22) Herndon, J. W.; Wang, H. *J. Org. Chem.* **1998**, *63*, 4564–4565.

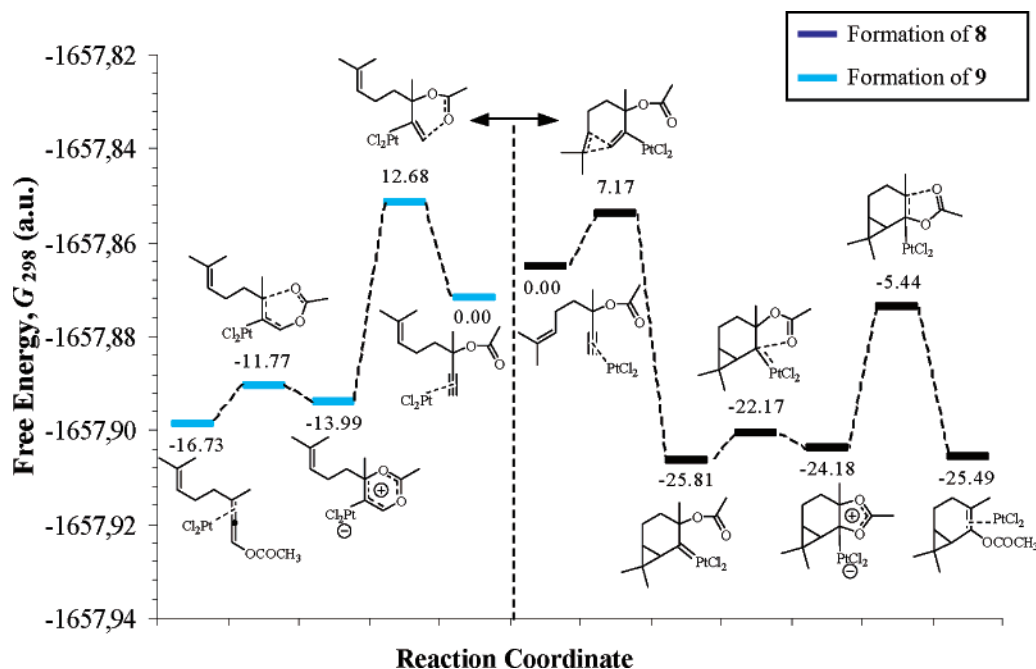


**Figure 1.** Free energy profiles computed for the PtCl<sub>2</sub>-catalyzed formation of **8** and **9** (free energy differences relative to the reactant complex are given in kcal mol<sup>-1</sup>).

vs 7.68 D for **11**) rather than to that involving the complete migration to C<sub>2</sub>. The simultaneous bonds of the acyloxy group with C<sub>2</sub> (O<sub>3</sub>-C<sub>2</sub> = 1.589 Å) and C<sub>3</sub> (O<sub>1</sub>-C<sub>3</sub> = 1.512 Å) in **12** give rise to a nearly planar oxacycle,<sup>23</sup> which allows an effective  $\pi$  delocalization. This second step is slightly endothermic (1.63 kcal mol<sup>-1</sup>), and the low activation energy (3.64 kcal mol<sup>-1</sup>) is consistent with the slight structural distortion required to reach **TS2**. Finally, **12** generates the enol ester by opening of the heterocycle. This transformation proceeds through **TS3** (O<sub>1</sub>-C<sub>3</sub> = 2.007 Å) with an activation barrier of 18.74 kcal mol<sup>-1</sup> (-5.44 kcal mol<sup>-1</sup> relative to **10**). The developed C<sub>2</sub>-C<sub>3</sub> double bond is  $\eta^2$  coordinated to the metal in an expected square-planar framework in the final adduct **8**-PtCl<sub>2</sub>.

These findings lead to the reaction energy profile depicted in Figure 1. The overall process is highly exothermic (-25.49 kcal mol<sup>-1</sup>), and the rate-limiting step is the opening of the oxacycle **12**, involving a moderate activation free energy.

Regarding path II, summarized in Scheme 3, the first step should involve an O-acyl migration to the  $\beta$ -carbon. We have verified that it would take place from an analogous  $\eta^2$ -alkyne reactant complex rather than from a slipped  $\eta^1$  complex,<sup>7</sup> which could not be located as a stable ground state. The nucleophilic attack at the internal alkyne carbon would lead to the polarized oxacycle **13** (12.1 D vs 5.0 D for the reactant complex) via **TS4** (O<sub>3</sub>-C<sub>2</sub> = 2.448 Å). It is remarkable that, although this step is also exothermic and proceeds with a moderately low activation free energy (9.51 kcal mol<sup>-1</sup>), **TS4** is about 2 kcal mol<sup>-1</sup> less stable than **TS1**, and **13** is about 4 kcal mol<sup>-1</sup> higher in energy than **11**; therefore, path I would be the preferred pathway from kinetic<sup>24</sup> and thermodynamic reasons. To obtain more

reliable energy values, single-point energy calculations were carried out at the B3LYP/6-311+G(2d,p)/LANL2DZ level, and we observed that the free energy difference between the two transition states rises slightly to 2.44 kcal mol<sup>-1</sup>.

However, in view of the small energy difference between **TS1** and **TS4**, and to gain further insights into this feasible mechanism, we determined the overall free energy profile for the proposal path II.<sup>25</sup> Accordingly, the vinyl platinacarbene **14** is formed by an easy cleavage of the O<sub>1</sub>-C<sub>3</sub> bond (via **TS5**), which may evolve through a cyclopropanation to the fused bicyclic adduct. The last transition structure, **TS6**, shows C<sub>1</sub>-C<sub>6</sub> (1.920 Å) and C<sub>1</sub>-C<sub>7</sub> distances (2.358 Å) closer than those computed for an initial 6-endo attack (path I); thus, we could presume a more significant steric hindrance due to substituents on the alkene. As expected, the energy barrier for this cyclization step (21.01 kcal mol<sup>-1</sup>) is higher than that for an initial 6-endo process.

To sum up, this plausible mechanism should proceed through three steps with low to moderate activation energy, the rate-limiting step involving a higher activation barrier than the alternative path I.

As we have discussed elsewhere,<sup>9</sup> the reactant complex under study presents a vacant coordination site around the metal, which might be occupied by an additional donor ligand such as a solvent molecule. Indeed, a more complete coordination sphere may induce energy changes. To get a deeper understanding about the role of an additional ligand, we performed calculations for the first step of paths I and II by incorporating H<sub>2</sub>O as a ligand.<sup>26</sup> In analogy with our previous obser-

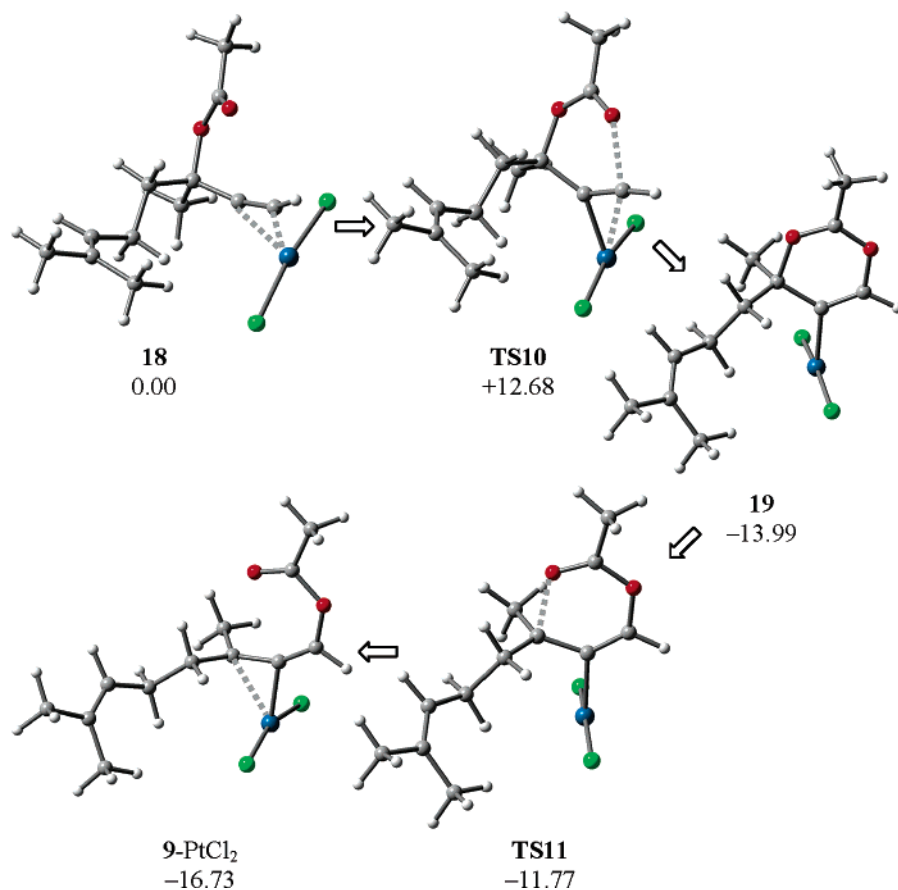
(23) Geometrical parameters: O<sub>1</sub>-C<sub>2</sub>-O<sub>3</sub>-C<sub>2</sub> = 11.16°; C<sub>2</sub>-O<sub>3</sub>-C<sub>2</sub>-C<sub>3</sub> = -15.09°; O<sub>3</sub>-C<sub>2</sub>-C<sub>3</sub>-O<sub>1</sub> = 13.27°; C<sub>2</sub>-C<sub>3</sub>-O<sub>1</sub>-C<sub>2</sub> = -9.03°; C<sub>3</sub>-O<sub>1</sub>-C<sub>2</sub>-O<sub>3</sub> = -1.24°.

(24) It could be argued that the lower electrophilic character at C<sub>2</sub> in the reactant complex (+0.04 vs +0.17 in **11**, Table S3; see the Supporting Information) would account for a less favorable electrostatic interaction with nucleophilic carbonyl oxygen and a higher energy transition state for acyl migration step as the first step.

(25) Optimized structures for this mechanistic proposal are given in the Supporting Information.



**Scheme 5. Optimized Structures for the Reaction Pathway of the PtCl<sub>2</sub>-Mediated Formation of 1-acetoxallene **9** from the 4-*O*-Acetyl-1,6-enyne **7****



vations, the formation of the Pt–carbene (path I) takes place with a higher activation energy for the coordinatively saturated system (11.54 vs 7.17 kcal mol<sup>-1</sup>). As has been proposed,<sup>9</sup> this effect could be attributed to the more effective back-donation from the metal into the  $\pi^*$  of the alkyne, which reduces the electrophilic activation. On the other hand, this step is similarly exothermic (–25.28 kcal mol<sup>-1</sup>). Interestingly, the free energy of activation for the initial 1,2-acyl migration (path II) is again about 2 kcal mol<sup>-1</sup> higher (13.43 kcal mol<sup>-1</sup>) than the formation of the Pt carbene (Scheme S2; see the Supporting Information).

Since **14** resembles a vinyl platinacarbene structure (Pt–C<sub>1</sub> = 1.910 Å), it might undergo an intramolecular [2 + 2] cycloaddition with the alkene (via **TS7**, not shown) to form the platina(IV)cyclobutane **15** (path III of Scheme 3), which could lead to the final bicyclic product (via **TS8**; not shown). However, this alternative route also entails a rather high energy barrier (26.32 kcal mol<sup>-1</sup>).<sup>8a</sup>

The mechanistic proposal suggested for the ZnCl<sub>2</sub>-catalyzed cycloisomerization of **7**<sup>11</sup> (path IV of Scheme 3) assumes the initial formation of a metal–alkene rather than a metal–alkyne  $\pi$  complex, **16**. The intramolecular trans attack of C<sub>1</sub> on the alkene carbon C<sub>6</sub> gives rise to **TS9**,<sup>25</sup> which displays a relatively short C<sub>1</sub>–C<sub>6</sub> bond (1.891 Å). IRC calculations confirm that this transition state affords the bicyclic intermediate **17** (path

IV of Scheme 3). This route implies an activation energy of 21.05 kcal mol<sup>-1</sup>, **TS9** being 9.33 kcal mol<sup>-1</sup> less stable than **TS1**. In addition, this step is less exothermic (–5.76 kcal mol<sup>-1</sup>) than formation of the fused bicycle **11**. Therefore, although the calculations were in agreement with the mechanistic proposal by Ohloff,<sup>11</sup> we also ruled it out as an active mechanism on the basis of kinetic and thermodynamic preferences.

In summary, our calculations suggest that path I should be the favored reaction path for the catalyzed formation of bicyclic enol esters from propargylic carboxylates.

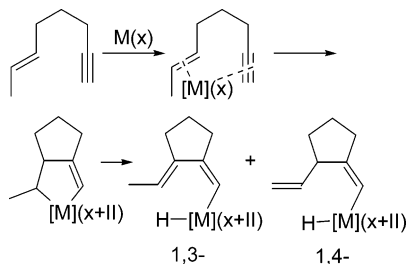
Experimental results indicate that, along with **8**, allene **9** is also isolated in low yield (Scheme 2);<sup>10</sup> therefore, our next goal was the elucidation of the reaction mechanism for this rearrangement. We proposed the structure **18** as the initial  $\eta^2$ -reactant complex, a more stable structure (4.13 kcal mol<sup>-1</sup>) than **10**, due to the less constrained alkyl chain. Starting from this structure, we located the transition state **TS10** (Scheme 5) by having the acyloxy group approach C<sub>1</sub> (O<sub>3</sub>–C<sub>1</sub> = 2.169 Å). **TS10** evolves to the polarized Pt–carbene **19** (11.57 D vs 4.55 D in **18**), showing a nearly planar six-membered heterocyclic structure.<sup>27</sup> This geometry allows an optimal orbital interaction and  $\pi$  delocalization.

The full migration of the acetyl group to C<sub>1</sub> takes place via **TS11**, by opening of the heterocycle (O<sub>1</sub>–C<sub>3</sub> = 2.084

(26) Despite this evaluation, the isomerizations under study were carried out in toluene, a solvent which has been proved to interact weakly with the Pt center.<sup>9</sup>

(27) Geometrical parameters: C<sub>3</sub>–O<sub>1</sub> = 1.603, O<sub>3</sub>–C<sub>1</sub> = 1.434 Å; dihedral angles O<sub>1</sub>–C<sub>6</sub>–O<sub>3</sub>–C<sub>1</sub> = –2.03°, C<sub>6</sub>–O<sub>3</sub>–C<sub>1</sub>–C<sub>2</sub> = 3.03°, O<sub>3</sub>–C<sub>1</sub>–C<sub>2</sub>–C<sub>3</sub> = 0.26°, C<sub>1</sub>–C<sub>2</sub>–C<sub>3</sub>–O<sub>1</sub> = –3.49°, C<sub>2</sub>–C<sub>3</sub>–O<sub>1</sub>–C<sub>6</sub> = 4.63°, C<sub>3</sub>–O<sub>1</sub>–C<sub>6</sub>–O<sub>3</sub> = –2.07°.

**Scheme 6. Reaction Pathway for the Pd-Catalyzed Generation of Alder-ene Type Products from 1,6-Enynes**



Å), and leads to the allenyl ester  $\eta^2$  complex **9**-PtCl<sub>2</sub>. The Pt–C<sub>2</sub> (2.003 Å) and Pt–C<sub>3</sub> (2.276 Å) distances imply  $\pi$  complexation onto the metal center, and the long C<sub>2</sub>–C<sub>3</sub> bond length (1.424 Å) reveals significant back-donation to the  $\pi^*$  orbital, resulting in a distorted allene structure (C<sub>1</sub>–C<sub>2</sub>–C<sub>3</sub> = 151.63°).

To sum up, the reaction proceeds through two exothermic steps (–13.99 and –2.75 kcal mol<sup>–1</sup>, respectively; see Figure 1), the first one being the rate-limiting step (12.68 kcal mol<sup>–1</sup>). Although the second step takes place with a very low energy barrier (2.22 kcal mol<sup>–1</sup>, –11.77 kcal mol<sup>–1</sup> relative to **18**), the [1,3]-acyl migration should be a stepwise rather than a concerted process. Remarkably,  $\pi$  coordination of alkyne onto the catalyst unvaryingly shows a Pt–C<sub>1</sub> distance that is shorter than the Pt–C<sub>2</sub> distance and a polarized C<sub>1</sub>–C<sub>2</sub> bond with an electrophilic center at the internal acetylenic carbon (Tables S3 and S6; see the Supporting Information). It should imply an unfavorable O<sub>3</sub>–C<sub>1</sub> electrostatic interaction and a subsequent difficult migration to C<sub>1</sub>. Calculated energy results show that **TS10** lies 1.38 kcal mol<sup>–1</sup> above **TS1**, and this energy difference should account for the experimental ratio of products.

Interestingly, formation of **8** is a more exothermic reaction than formation of **9** (–25.49 vs –16.73 kcal mol<sup>–1</sup>) and the major bicyclic product is 4.62 kcal mol<sup>–1</sup> more stable than the allenyl ester. Hence, the PtCl<sub>2</sub>-mediated cycloisomerization of **8** is the favored process from both kinetic and thermodynamic viewpoints. Figure 1 depicts and quantitatively compares the absolute energy profiles computed for both reactions.

It is well-known that transition-metal complexes catalyze the cyclization of enynes to give the Alder-ene product (1,4-diene).<sup>4a,28,29</sup> To justify and understand the absence of this product, under the reaction conditions, we have carried out a mechanistic study of this alternative cycloisomerization. Accordingly, we have analyzed the mechanistic proposal suggested by Trost and Lautens<sup>29</sup> (Scheme 6), which involves an oxidative cyclization,  $\beta$ -H elimination, and reductive elimination steps.<sup>30</sup>

The coordination of catalyst to unsaturated ligands of the enyne forms the  $\eta^4$  complex **20** (see Scheme 7 and

Table S9 in the Supporting Information). Oxidative cyclization affords the platinumacyclopentene **21** through **TS12** (C<sub>2</sub>–C<sub>6</sub> = 2.151 Å). The chelate complex **21** shows a trans arrangement of chloride ligands and an octahedral coordination framework with the trans positions to  $\sigma$  Pt–alkenyl and  $\sigma$  Pt–alkyl bonds vacant. The bite angle (C<sub>1</sub>–Pt–C<sub>7</sub>) is 82.20°, slightly distorted from the ideal octahedral arrangement. This oxidative cyclization step takes place with a moderately high activation energy (35.39 kcal mol<sup>–1</sup>; see Figure 2 and Table S10 in the Supporting Information) and is exothermic by –13.93 kcal mol<sup>–1</sup>. These results are significantly less favorable than those previously reported by Echavarren et al. at the same theoretical level for the simple enyne (30.1 and –23.6 kcal mol<sup>–1</sup>, respectively),<sup>6d</sup> probably due to steric effects arising from propargylic substituents.

Since an exhaustive description of the overall transformation is beyond the scope of this essay, we focus herein on the most remarkable conclusions we have found from this study.<sup>31</sup> Our calculations were in perfect agreement with the mechanistic pathway advanced in Scheme 6 and showed that the rate-limiting step should be the oxidative cyclization step. Furthermore, the transition structure **TS12** suggests that a quaternary propargylic center may cause congestion in the course of the catalyst approach. Consequently, the cyclometalation could be inhibited or retarded, as it can be confirmed from comparison between energy values for simple and substituted 1,6-enynes related above. In other words, the bulkier the substituents at the propargylic position, the more congested the transition structure and the more difficult the cyclometalation. Under these conditions, a complete change in mechanism could be observed, affording alternative cycloisomerization products.<sup>32</sup>

In light of the computed results for the Alder-ene reaction and those for formation of enol ester **8** and allene **9**, some relevant conclusions can be drawn. Since the Alder-ene adduct is the most stable of the calculated products (compare Tables S2, S5, and S10 in the Supporting Information), the product ratio observed experimentally should be due to kinetic factors. For the three types of reaction mechanisms described above, the calculated results indicate that the first transition structure is the highest energy stationary point along the reaction energy profile. Notably, the formation of enol ester **8** involves the lowest energy transition state, **TS1**, while formation of allene implies a transition structure 1.4 kcal mol<sup>–1</sup> above and the Alder-ene product 10.7 kcal mol<sup>–1</sup> above **TS1**. These findings are consistent with experimental data and suggest that the product ratio in these catalytic processes could be mainly attributed to a kinetic preference induced by the propargylic substituent.

Finally, we extended our analysis to the dienyne precursor **24** to get theoretical insights into the effect of an additional alkenyl ligand (Scheme 8). As shown in Scheme 1, the presence of two lateral alkene groups may provide two bicyclo [*n*.1.0] enol esters as cyclo-

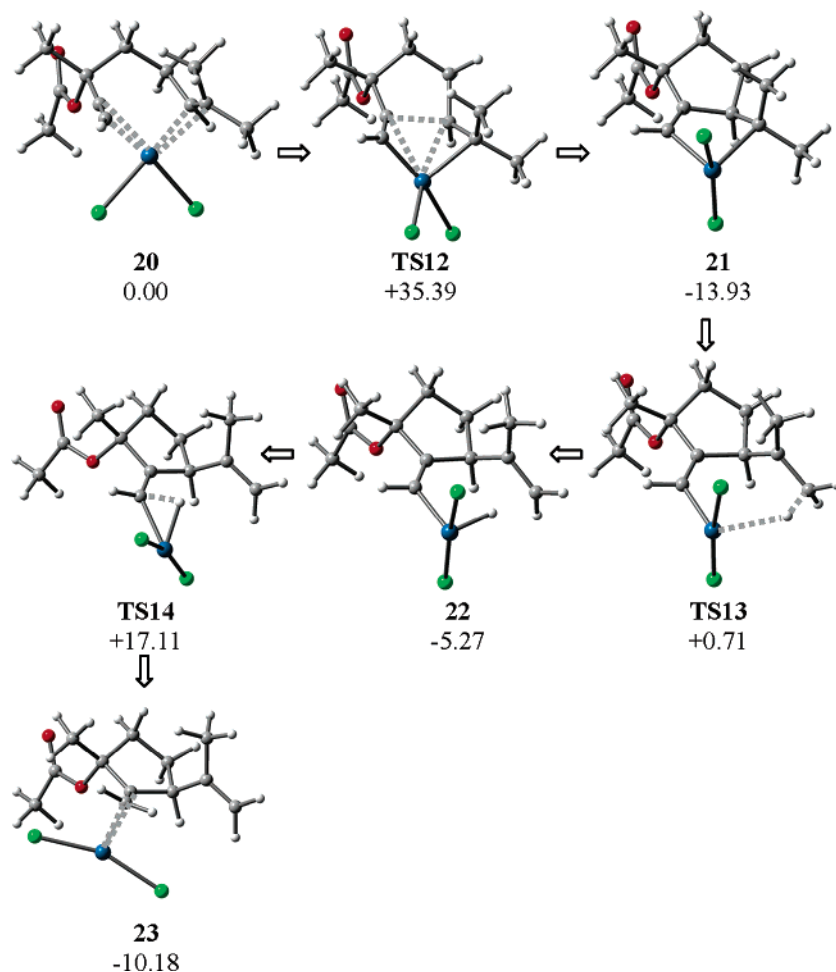
(28) Trost, B. M.; Lautens, M. *J. Am. Chem. Soc.* **1985**, *107*, 1781–1783.

(29) Trost, B. M.; Tanoury, G. J.; Lautens, M.; Chan, C.; Macpherson, D. T. *J. Am. Chem. Soc.* **1994**, *116*, 4255–4267.

(30) This mechanism has also been proposed by other authors. (a) For Rh(I)-catalyzed cycloisomerization of enynes for the preparation of functionalized lactams, see ref 5c. (b) For Ti(II)-catalyzed cyclizations, see: Sturla, S. J.; Kablaoui, N. M.; Buchwald, S. L. *J. Am. Chem. Soc.* **1999**, *121*, 1976–1977. (c) For cycloisomerization with PtCl<sub>2</sub>, see ref 6d. (d) For cycloisomerization with [CpRu(MeCN)<sub>3</sub>][PF<sub>6</sub>], see: Trost, B. M.; Toste, F. D. *J. Am. Chem. Soc.* **2000**, *122*, 714–715.

(31) A detailed analysis of the overall mechanism, which also accounts for the preferential abstraction of hydrogen from the trans allylic position in the intermediate **21**, is provided as part of the Supporting Information.

(32) Trost, B. M.; Toste, F. D. *J. Am. Chem. Soc.* **2002**, *124*, 5025–5036.

**Scheme 7. Optimized Structures for the Reaction Pathway of the PtCl<sub>2</sub>-Mediated Intramolecular Cycloisomerization of 1,6-Enyne **7** to the Alder-ene Product**

isomerization products, suggesting the same operative mechanism. On the basis of the mechanistic picture proposed for the formation of **8** (Scheme 4), we computed the energy profile for both cyclohexene (**28**) and cyclopentene (**32**) derivatives (Table 1). In comparison with the enyne, the formation of the cyclohexyl platinumcarbene intermediate **26** is a more exothermic step due to the lesser steric hindrance of the unsubstituted fused cyclopropane, which indeed could also account for a thermodynamically favored overall process ( $-25.49$  kcal mol<sup>-1</sup> for *gem*-dimethyl enyne vs  $-30.75$  kcal mol<sup>-1</sup> for unsubstituted enyne).

As we have reported for a related free alcohol derivative,<sup>9</sup> the presence of the pendant alkene chain could affect the nature and stability of the intermediate structures (Table 1). As expected, additional  $\pi$  complexation of the remote alkene leads to more stable structures along the reaction path (for instance, the  $\eta^4$  reactant complex is  $19.96$  kcal mol<sup>-1</sup> lower in energy than the coordinatively unsaturated  $\eta^2$  complex). Nevertheless, the formation of the platinumcarbene **26**( $\eta^4$ ) proceeds with a higher activation barrier. These results, parallel to those described for the 5-exo and 6-endo cyclization of the alcohol precursor,<sup>9</sup> reveal that additional complexation stabilizes the stationary structures along the reaction path due to a more effective  $\pi$  back-bonding interaction that, indeed, results in a less enhanced electrophilic character of the coordinated alkyne (NPA charges  $-0.214$  vs  $-0.184$  for C<sub>1</sub> in the  $\eta^4$

and  $\eta^2$  complexes, respectively). The energy profile remains qualitatively equivalent.

The cycloisomerization should proceed through a 6-endo cyclopropanation followed by a stepwise [1,2]-acyl migration, involving low activation barriers. The reaction is largely favored from a thermodynamic perspective ( $-24.06$  kcal mol<sup>-1</sup>), and the rate-limiting step should be the cyclopropanation. The optimized structures are depicted in Scheme 9.

On the other hand, the formation of **32** shows some remarkable energy differences (see Scheme S4 in the Supporting Information). The initial 5-endo cyclization implies an activation energy ( $17.21$  kcal mol<sup>-1</sup>) considerably higher than that estimated for the 6-endo attack ( $11.17$  kcal mol<sup>-1</sup>) and is less exothermic ( $-13.21$  vs  $-21.26$  kcal mol<sup>-1</sup>), due to a higher annular tension of the substituted intermediate. In comparison with the formation of **28**, the formation of the bicyclo[3.1.0]hexane framework leads to less stable structures along the reaction path, whereas the activation barriers for the [1,2]-acyl migration show similar values. This results leads to a less exothermic formation of **32** ( $-16.79$  kcal mol<sup>-1</sup>) with respect to **28** ( $-24.06$  kcal mol<sup>-1</sup>).

## Conclusions

In this paper we present additional mechanistic insights into the transition-metal-mediated cycloisomer-

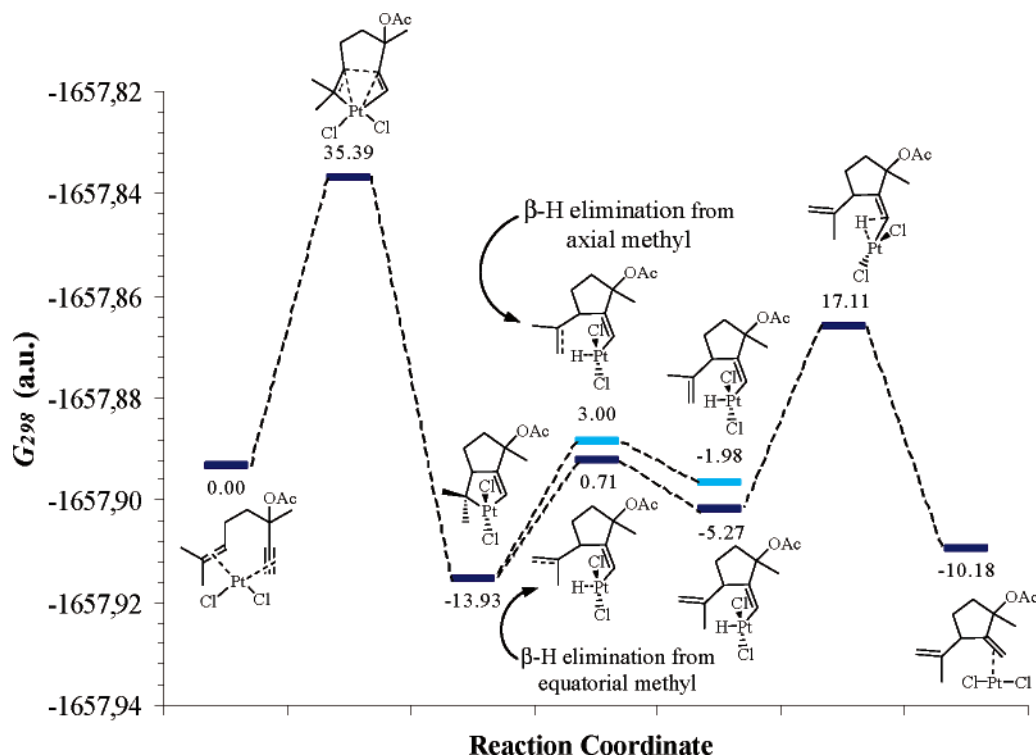
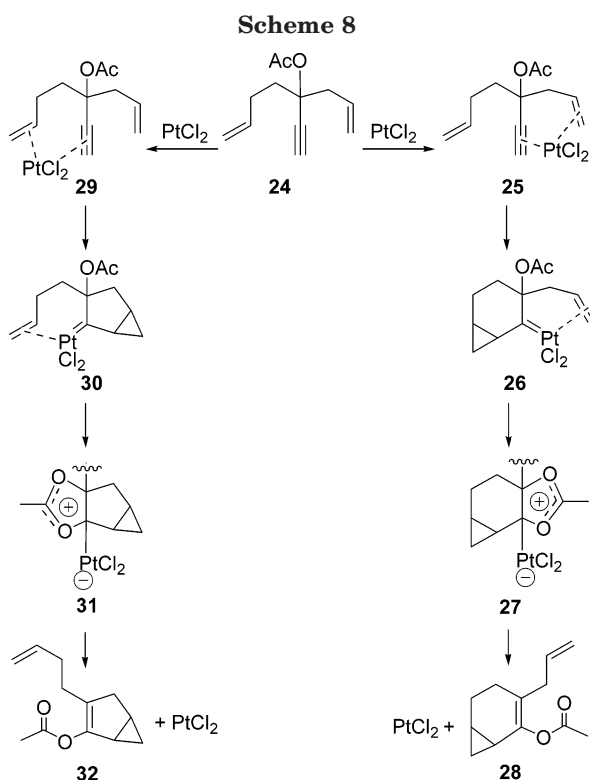


**Figure 2.** Free energy profile for the Alder-ene reaction (free energy differences relative to the reactant complex are given in kcal mol<sup>-1</sup>).



ization of 1,6-enynes bearing propargylic substituents. As a complement to further studies,<sup>9</sup> we report herein the reaction pathway for the Pt(II)-mediated cycloisomerization of propargylic carboxylates, which can yield bicyclo [n.1.0] enol esters.

The coordination of the alkyne to electrophilic PtCl<sub>2</sub> activates the intramolecular nucleophilic attack by the tethered alkene and leads to the key Pt-carbene intermediates **a** and **b**, through exo and endo cyclopro-

**Table 1.** Total<sup>a</sup> and Free<sup>b</sup> Energy Differences Computed for PtCl<sub>2</sub>-Mediated Cycloisomerization of **24**

	η <sup>2</sup> complex		η <sup>4</sup> complex		η <sup>4</sup> complex		
	ΔE (kcal mol <sup>-1</sup> )	ΔG <sub>298</sub> (kcal mol <sup>-1</sup> )	ΔE (kcal mol <sup>-1</sup> )	ΔG <sub>298</sub> (kcal mol <sup>-1</sup> )	ΔE (kcal mol <sup>-1</sup> )	ΔG <sub>298</sub> (kcal mol <sup>-1</sup> )	
<b>25</b>	0.00	0.00	0.00	0.00	<b>29</b>	0.00	0.00
<b>TS15</b>	+5.65	+7.02	+9.75	+11.17	<b>TS18</b>	+17.39	+17.21
<b>26</b>	-35.71	-33.40	-23.67	-21.26	<b>30</b>	-14.48	-13.21
<b>TS16</b>	-34.09	-30.62	-21.51	-18.04	<b>TS19</b>	-12.11	-9.35
<b>27</b>	-35.31	-31.51	-24.12	-20.70	<b>31</b>	-12.65	-10.25
<b>TS17</b>	-23.26	-20.00	-13.88	-10.38	<b>TS20</b>	-1.71	+1.09
<b>28</b>	-33.84	-30.75	-25.35	-24.06	<b>32</b>	-18.44	-16.79

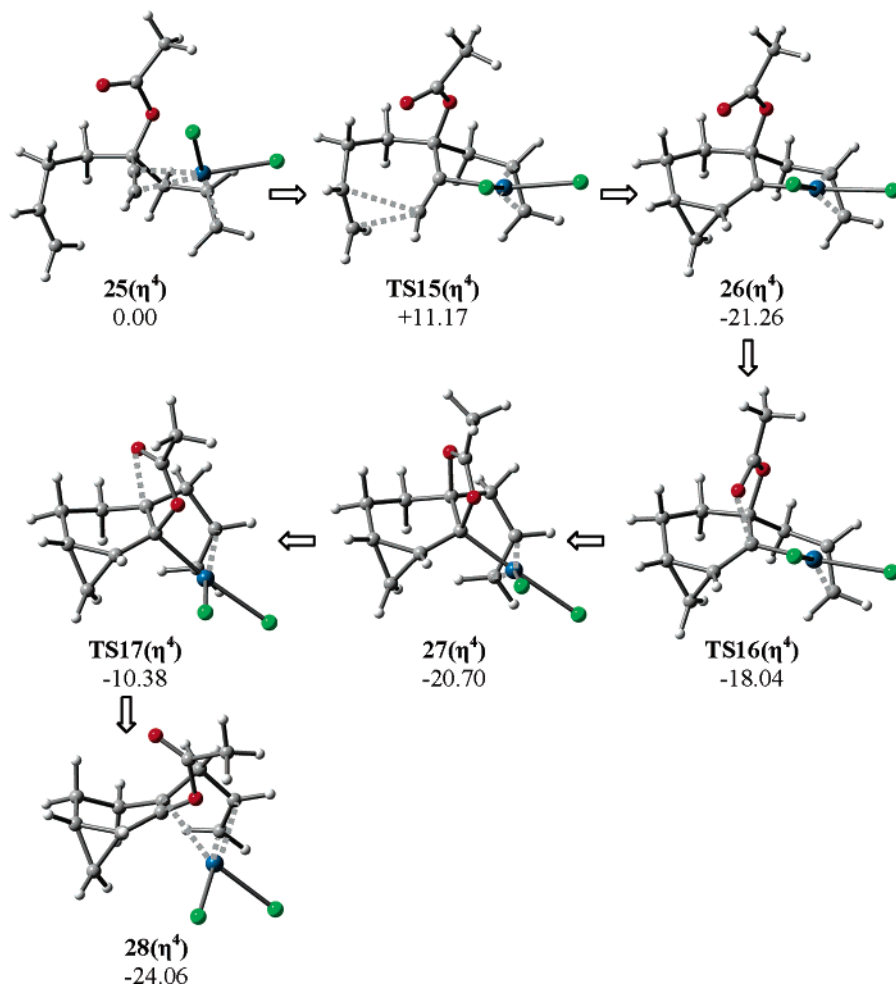
<sup>a</sup> Zero-point corrected values. <sup>b</sup> Includes thermal corrections at 298 K.

panation steps, respectively (Scheme 10), which may evolve through different pathways depending on the molecular structure. The selection of the initial cyclization mode is governed by the precursor structure. Formation of the intermediate **a** should be the common path for the formation of the metathesis adduct (**d**) and functionalized polycyclic structures (**e**).<sup>9</sup> In contrast, the propargylic O-acyl protecting group in simple enyne or dienyne induces the formation of bicyclic enol ester(s) **f** through an initial endo attack, followed by a stepwise [1,2]-acyl migration. In these cases, the bulky propargylic substituent inhibits other cycloisomerization reactions, such as an exo-cyclization route or the Alder-ene process (**h**), and the easy [1,2]-acyl migration by anchimeric assistance promotes the formation of bicyclic [n.1.0] enol esters.

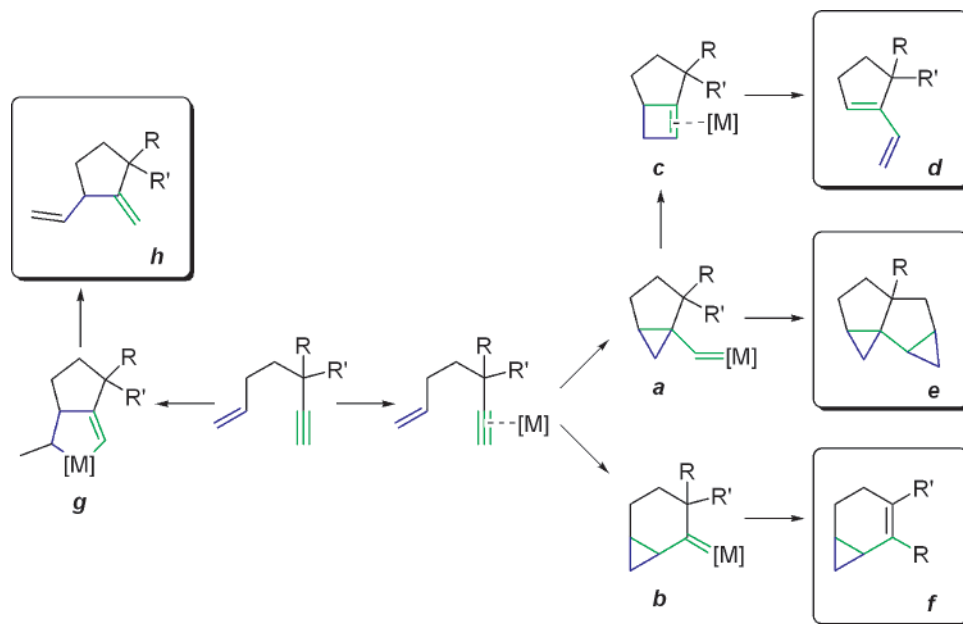
In summary, these findings provide new mechanistic details about the PtCl<sub>2</sub>-mediated isomerizations of enynes and the origin of the chemo-, regio-, and stereo-selectivity.



**Scheme 9. Optimized Structures for the PtCl<sub>2</sub>-Mediated Formation of Bicyclic Enol Ester from Dienyne 24**



**Scheme 10. PtCl<sub>2</sub>-Mediated Cycloisomerization of 1,6-Enynes**



**Computational Methods**

Calculations have been carried out using the Gaussian03 program.<sup>33</sup> The geometries have been fully optimized at the DFT level by means of the B3LYP hybrid functional.<sup>34</sup> Pt

has been described by the LANL2DZ basis set,<sup>35</sup> where the innermost electrons are replaced by a relativistic ECP and the 18 valence electrons are explicitly treated by a double- $\zeta$  basis set. For all other atoms, the 6-31G(d) basis set has been employed.

Harmonic frequencies were calculated at the optimization level, and the nature of the stationary points was determined in each case according to the right number of negative eigenvalues of the Hessian matrix. The intrinsic reaction coordinate (IRC) pathways<sup>36a</sup> from the transition structures have been followed using a second-order integration method,<sup>36b</sup> to verify the expected connections of the first-order saddle points with the correct local minima found on the potential energy surface. Zero-point vibration energy (ZPVE) and ther-

mal corrections (at 298 K) to the energy have been estimated on the basis of the frequency calculations at the optimization level and scaled by the recommended factor.

To obtain more reliable energy values, some single-point energy calculations at the B3LYP/6-311+G(2d,p)/LANL2DZ level were carried out on the B3LYP/6-31G(d)/LANL2DZ geometries. The results revealed a negligible basis set effect.

Natural bond orbital (NBO) analyses<sup>37</sup> have been performed at the DFT level by the module NBO v.3.1 implemented in Gaussian03, in order to evaluate the NPA atomic charges and delocalization interactions.

**Supporting Information Available:** Text, tables, and figures giving results for the calculations of the cycloisomerization reactions and of the alternative mechanistic proposals evaluated throughout this study, including a detailed analysis of the Alder-ene reaction pathway, and atomic coordinates for computed structures. This material is available free of charge via the Internet at <http://pubs.acs.org>.

OM050134R

(33) Frisch, M. J.; Trucks, G. W.; Schlegel, H. B.; Scuseria, G. E.; Robb, M. A.; Cheeseman, J. R.; Montgomery, Jr., J. A.; Vreven, T.; Kudin, K. N.; Burant, J. C.; Millam, J. M.; Iyengar, S. S.; Tomasi, J.; Barone, V.; Mennucci, B.; Cossi, M.; Scalmani, G.; Rega, N.; Petersson, G. A.; Nakatsuji, H.; Hada, M.; Ehara, M.; Toyota, K.; Fukuda, R.; Hasegawa, J.; Ishida, M.; Nakajima, T.; Honda, Y.; Kitao, O.; Nakai, H.; Klene, M.; Li, X.; Knox, J. E.; Hratchian, H. P.; Cross, J. B.; Bakken, V.; Adamo, C.; Jaramillo, J.; Gomperts, R.; Stratmann, R. E.; Yazyev, O.; Austin, A. J.; Cammi, R.; Pomelli, C.; Ochterski, J. W.; Ayala, P. Y.; Morokuma, K.; Voth, G. A.; Salvador, P.; Dannenberg, J. J.; Zakrzewski, V. G.; Dapprich, S.; Daniels, A. D.; Strain, M. C.; Farkas, O.; Malick, D. K.; Rabuck, A. D.; Raghavachari, K.; Foresman, J. B.; Ortiz, J. V.; Cui, Q.; Baboul, A. G.; Clifford, S.; Cioslowski, J.; Stefanov, B. B.; Liu, G.; Liashenko, A.; Piskorz, P.; Komaromi, I.; Martin, R. L.; Fox, D. J.; Keith, T.; Al-Laham, M. A.; Peng, C. Y.; Nanayakkara, A.; Challacombe, M.; Gill, P. M. W.; Johnson, B.; Chen, W.; Wong, M. W.; Gonzalez, C.; Pople, J. A. *Gaussian 03*, Revision B.03; Gaussian, Inc., Wallingford, CT, 2004.

(34) (a) Lee, C.; Yang, W.; Parr, R. *Phys. Rev. B* **1988**, *37*, 785–789. (b) Becke, A. *J. Chem. Phys.* **1993**, *98*, 5648–5652.

(35) Hay, P. J.; Wadt, W. R. *J. Chem. Phys.* **1985**, *82*, 270–283.

(36) (a) Fukui, K. *Acc. Chem. Res.* **1981**, *14*, 363–368. (b) González, C.; Schlegel, H. B. *J. Phys. Chem.* **1990**, *94*, 5523–5527.

(37) (a) Reed, A. E.; Weinhold, F. *J. Chem. Phys.* **1983**, *78*, 4066–4073. (b) Reed, A. E.; Curtiss, L. A.; Weinhold, F. *Chem. Rev.* **1988**, *88*, 899–926.